Monthly Notices
of the
ROYAL ASTRONOMICAL SOCIETY

MNRAS **465,** L79–L83 (2017)
Advance Access publication 2016 October 20

doi:10.1093/mnrasl/slw214

The origin of type I profiles in cluster lenticulars: an interplay between ram pressure stripping and tidally induced spiral migration

Adam J. Clarke,[1]★ Victor P. Debattista,[1] Rok Roškar[2] and Tom Quinn[3]

[1]*Jeremiah Horrocks Institute, University of Central Lancashire, Preston PR1 2HE, UK*
[2]*Research Informatics, Scientific IT Services, ETH Zürich, Weinbergstrasse 11, CH-8092 Zürich, Switzerland*
[3]*Astronomy Department, University of Washington, Box 351580, Seattle, WA 98195, USA*

Accepted 2016 October 11. Received 2016 October 11; in original form 2016 July 28

ABSTRACT

Using *N*-body + smooth particle hydrodynamics simulations of galaxies falling into a cluster, we study the evolution of their radial density profiles. When evolved in isolation, galaxies develop a type II (down-bending) profile. In the cluster, the evolution of the profile depends on the minimum cluster-centric radius the galaxy reaches, which controls the degree of ram pressure stripping. If the galaxy falls to ∼50 per cent of the virial radius, then the profile remains type II, but if the galaxy reaches down to ∼20 per cent of the virial radius, the break weakens and the profile becomes more type I like. The velocity dispersions are only slightly increased in the cluster simulations compared with the isolated galaxy; random motion therefore cannot be responsible for redistributing material sufficiently to cause the change in the profile type. Instead, we find that the joint action of radial migration driven by tidally induced spirals and the outside-in quenching of star formation due to ram pressure stripping alters the density profile. As a result, this model predicts a flattening of the age profiles amongst cluster lenticulars with type I profiles, which can be observationally tested.

Key words: galaxies: clusters: general – galaxies: elliptical and lenticular, cD – galaxies: evolution – galaxies: formation – galaxies: spiral.

1 INTRODUCTION

Lenticular (S0) galaxies share the discy morphology of spirals, but are red and dead, with a lack of young stars and a smooth appearance which results from an absence of a substantial amount of cold gas (e.g. Chamaraux, Balkowski & Fontanelli 1986). They tend to be found more frequently in clusters, while the field environment favours spiral galaxies (Dressler 1980; Cappellari et al. 2011). The fraction of lenticulars decreases with redshift, while that of spirals increases (Dressler et al. 1997; Couch et al. 1998; Postman et al. 2005), implying that lenticular galaxies form via the transformation of spirals. Various mechanisms have been proposed to explain the quenching of their star formation (SF). Ram pressure stripping (RPS) can remove the majority of cool gas (Gunn & Gott III 1972; Quilis 2000) or the hot gas corona, preventing future gas cooling on to the disc and ending a galaxy's ability to form stars, often referred to as strangulation (Larson, Tinsley & Caldwell 1980; Bekki, Couch & Shioya 2002; Steinhauser, Schindler & Springel 2016). Harassment (Moore et al. 1996, 1999) and minor-merger-triggered starbursts leading to gas depletion (Mihos & Hernquist 1994; Bekki 1998) can also quench SF. It is not yet clear which of these mechanisms dominates.

It has long been known that the bright parts of disc galaxies show an exponentially declining surface density (Freeman 1970). However, most profiles have a change in scalelength at a 'break-radius'. Freeman (1970) defines two disc profile types. The first, type I profiles, are purely exponential out to the last measured point (for example in NGC 300 this extends to 10 scalelengths, Bland-Hawthorn et al. 2005; Erwin, Pohlen & Beckman 2008; Vlajić, Bland-Hawthorn & Freeman 2011). Type II profiles instead show a decrease in scalelength past a break-radius. These breaks have been shown to originate from a drop in the star formation rate (SFR; Schaye 2004; Roškar et al. 2008a; Radburn-Smith et al. 2012). The outer disc is then populated by stars migrating outward due to transient spiral structure, via the corotation resonance trapping mechanism proposed by Sellwood & Binney (2002). This leads to a type II profile with a break-radius which moves outwards as gas cools on to the disc (Roškar et al. 2008a). Alternatively, type II profiles have also been explained without an SF threshold, via angular momentum exchanges mediated by bars and spirals (Debattista et al. 2006; Foyle, Courteau & Thacker 2008; Minchev & Famaey 2010), although this leads to hot outer discs. Galaxies with type II profiles exhibit an upturn in their colour profile close to the break-radius (Azzollini, Trujillo & Beckman 2008; Bakos, Trujillo

★ E-mail: aclarke13@uclan.ac.uk

& Pohlen 2008). A third type of profile, termed type III, shows an increase in scalelength past the break-radius (Erwin, Beckman & Pohlen 2005). Type III profiles are generally thought to result from heating of the inner disc through various mechanisms (e.g. Younger et al. 2007; Minchev et al. 2012; Borlaff et al. 2014; Herpich et al. 2015).

Erwin, Gutiérrez & Beckman (2012) studied the distribution of light profiles amongst lenticular galaxies. They found that the fraction of type I and II profiles depends on the environment. Amongst the field lenticulars, type I and type II profiles were equally common. However, they found virtually no type II profiles amongst cluster lenticulars and double the frequency of type I profiles. Roediger et al. (2012) also found no type II profiles amongst Virgo lenticulars. Gutiérrez et al. (2011) found that 33 per cent of their sample of lenticulars, but only 10 per cent of spirals, showed a type I profile, and that the frequency of type II profiles changes from 80 per cent to 25 per cent for the spiral and lenticular samples, respectively. Pranger et al. (2016) constructed two samples of galaxies with mass $1-4\times10^{10}$ M$_\odot$, one in the field and one in the cluster environment. Comparing the profiles, they found that type I profiles are three times more frequent in clusters than in the field. Because they considered the outer discs, at surface brightness $24<\mu<26.5$ mag arcsec^{-2}, beyond where most disc breaks are located (Pohlen & Trujillo 2006), Maltby et al. (2015) found remarkably similar frequencies of type I/II/III profiles amongst lenticulars in the cluster and field environments. They also found no difference in disc scalelengths between lenticular and spiral galaxies. These studies imply that environmental processes driving the evolution of lenticulars may also be responsible for the light-profile properties, which may provide insight into which cluster lenticular formation mechanism is most important. Herpich et al. (2015) demonstrated that pure exponential discs occur in simulations when the halo has a narrow range of angular momentum, potentially explaining how isolated galaxies can exhibit single-exponential profiles.

In this Letter, we use N-body + smooth particle hydrodynamics (SPH) simulations of spiral galaxies falling into a cluster where they experience RPS, substantially quenching their SF. We consider the evolution of the density profiles compared with the same galaxy evolved in isolation and demonstrate that the mechanism driving the differences is radial migration enhanced by tidally induced spirals, with RPS playing a vital role by quenching SF outside-in.

2 SIMULATIONS

Our simulations consist of single galaxies falling into a cluster. The initial conditions for the galaxy are the same as those used in the well-studied system of Roškar et al. (2008a,b) and Loebman et al. (2011), with a spherical NFW dark matter halo (Navarro, Frenk & White 1995) and an embedded spherical corona of gas with a temperature profile such that hydrostatic equilibrium is established. We impart an angular momentum, $j\propto R$, to the gas, with a spin parameter of $\lambda=0.065$ (Bullock et al. 2001). The dark matter consists of two shells, the inner containing 9×10^5 particles of mass 10^6 M$_\odot$ extending to 200 kpc and the outer containing 1×10^5 particles of mass 3.5×10^6 M$_\odot$. There are 10^6 gas particles, each with mass 1.4×10^5 M$_\odot$. The total mass within the virial radius ($R_{200}=200$ kpc) is 10^{12} M$_\odot$. We use a softening of 50 pc for the gas and stars, and 100 pc for the dark matter.

We consider a cluster similar in size and mass to the Fornax cluster. The virial radius is set to 0.7 Mpc and the virial mass enclosed is 6×10^{13} M$_\odot$ (Ikebe et al. 1992; Drinkwater, Gregg & Colless 2001; Nasonova, de Freitas Pacheco & Karachentsev 2011). We model the cluster with 9×10^6 dark matter particles of mass 4×10^6 M$_\odot$ in the inner shell, extending to 700 kpc, and 10^6 dark matter particles of mass 2×10^7 M$_\odot$ in the outer shell. There are 2×10^7 gas particles in the cluster, each of mass 2.3×10^5 M$_\odot$ producing a mass resolution comparable to that in the galaxy itself. The softening lengths are set to match the infalling galaxy. We prevent the cluster gas from cooling, to mimic the episodic active galactic nucleus feedback, which prevents substantial SF in the centres of massive clusters (Binney 2004).

We initially place the galaxies at three times the cluster virial radius, to allow the galaxy to form a disc before RPS commences. Here, we present just two simulations, which we refer to as 'cluster350' and 'cluster150', targeting periapsis at 350 and 150 kpc, respectively. With the cluster centred on the origin, we place the galaxies along the z-axis from the cluster centre, with the internal angular momentum vector also along the z-axis and the orbital angular momentum vector perpendicular to it, i.e. along the x-axis. We give the cluster150 model velocities $v_y=273$ km s^{-1} and $v_z=157$ km s^{-1}, whilst the cluster350 model has $v_y=157$ km s^{-1} and $v_z=273$ km s^{-1}. We use the isolated simulation of Loebman et al. (2011) as a control model to disentangle the effect of environment and refer to this simulation as the 'isolated' model.

We evolve the models for 10 Gyr with the N-body + SPH code GASOLINE (Wadsley, Stadel & Quinn 2004). We adopt SF criteria where the gas density and temperature have to be greater than 0.1 cm^{-3} and less than 15 000 K, respectively. Feedback from both Type II and Type Ia supernovae is introduced via energy injected into the interstellar medium in the form of a sub-grid modelled blastwave as described in Stinson et al. (2006). Stars form with one-third of the gas particle mass, corresponding to 4.6×10^4 M$_\odot$, and each gas particle can form multiple stellar particles. The minimum gas mass is set at one-fifth of its original mass. Once a gas particle drops below this mass, it is removed, and its mass is distributed to the surrounding gas particles. We adopt a base time-step of $\Delta t=0.01$ Gyr, refining our time-steps using $\delta t=\Delta t/2^n<\eta(\epsilon/a_g)^{1/2}$, where ϵ is the softening length and a_g is the particle acceleration at the current position. We set the refinement parameter $\eta=0.175$. The tree code opening angle $\theta=0.7$. The time-step for gas particles also satisfies $\delta t_{\rm gas}=\eta_{\rm courant}h/[(1+\alpha)c+\beta\mu_{\rm max}]$, where h is the SPH smoothing length, $\eta_{\rm courant}=0.4$, $\alpha=1$ is the shear coefficient, $\beta=2$ is the viscosity coefficient and $\mu_{\rm max}$ is described in Wadsley et al. (2004). The SPH kernel is defined using the nearest 32 neighbours. These parameters have been shown to lead to realistic late-type galaxies (Roškar et al. 2012; Roškar, Debattista & Loebman 2013).

3 RESULTS

In the top panel of Fig. 1, we show the evolution of the mass within the inner 10 kpc of the cluster150 model compared with the isolated galaxy. Initially, the cluster150 and isolated models evolve in parallel. At ∼4 Gyr, the galaxy reaches a location in the cluster dense enough for RPS of the cool gas to become strong, which occurs around the time of periapsis. The bottom panel shows the SF histories for all three models. In the cluster galaxies, prior to significant mass-loss, there is a burst of SF, which we attribute to compression of the cool gas by the cluster medium. This is strongest in the cluster150 model, but a milder one is also apparent in the cluster350 model. SF in the latter model is quenched much more gently, but by 10 Gyr it is forming stars at roughly half the rate (∼2 M$_\odot$ yr^{-1}) of the isolated model. The cluster150 model terminates SF almost entirely, except in the very inner ($\lesssim$1 kpc)

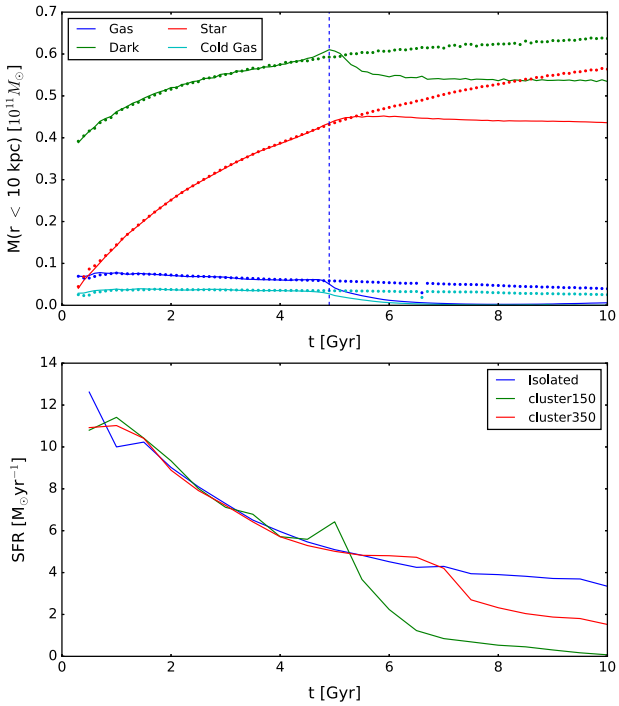

Figure 1. Top panel: evolution of the mass enclosed within the inner 10 kpc in the cluster150 galaxy (solid) compared with the isolated galaxy (dotted). The blue line shows all gas particles whilst the cyan line shows only cool ($T < 15\,000$ K) gas. Green and red show the dark matter and stellar content, respectively. The vertical lines correspond to the time at which the cluster150 galaxy is at periapsis. Bottom panel: SF histories for our models, as detailed at top right.

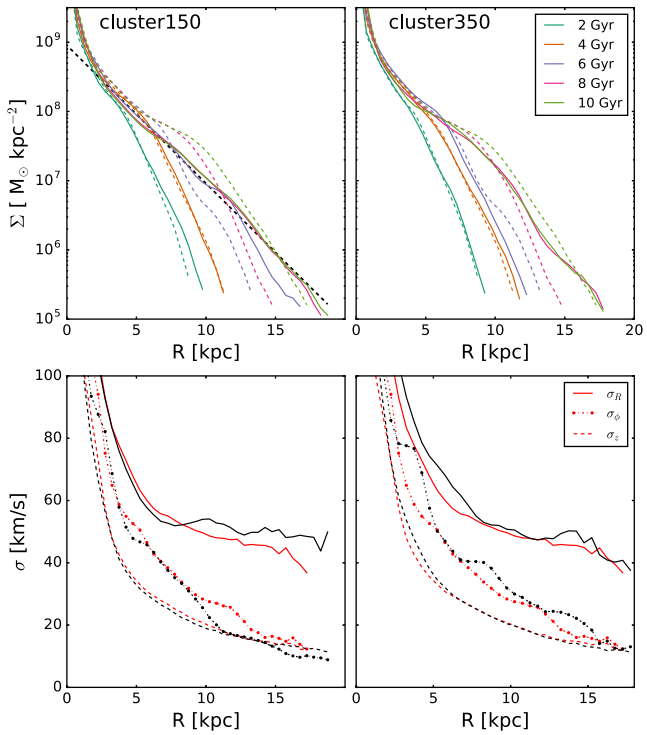

Figure 2. Top panel: evolution of the surface density profiles for the cluster150 (left) and cluster350 (right) models (solid lines) compared with the isolated model (dashed lines) as detailed on the right. The black dashed line shows a single-exponential fit to the disc component of the 10 Gyr cluster150 model. Bottom panel: final velocity dispersion profiles for the cluster galaxies (black lines) compared with the isolated simulation (red lines).

regions. A small ($\lesssim$10 per cent) fraction of dark matter is also lost from the inner 10 kpc.

In the top panels of Fig. 2, we compare the evolution of the surface density profiles of the isolated and the cluster galaxies. The isolated galaxy develops a type II profile due to the SF drop and outwardly migrating stars moving past the break-radius (Roškar et al. 2008a). At early times the cluster150 galaxy (left-hand panel) exhibits a type II profile, with the break moving outwards, initially evolving identically to the isolated galaxy. Once the galaxy is approaching periapsis and RPS is strongest, it begins to transition from a type II to a type I profile. It is noteworthy that in the final profiles the main difference between the isolated and cluster150 models is not at large radii, but at intermediate ($\sim$7–10 kpc) radii. At 8 Gyr, the outer disc of the cluster350 model is more massive than that of the isolated model. By 10 Gyr the break in the profile is weaker, but it retains a type II profile.

Fig. 3 shows the surface density profiles of young stars (age <0.5 Gyr) as a function of radius. In the isolated model, SF grows inside-out as more gas cools on to the disc. In comparison, the cluster150 model grows inside-out only up to the onset of RPS, at which point the SF quenches from the outside-in. Significant SF never extends beyond $\sim$6 kpc; the disc therefore never has an opportunity to form a substantial mass beyond this point. This explains why the difference between the profiles of the cluster150 and isolated models is largest at these intermediate radii, i.e. between the maximum extent of SF in the cluster150 model and the final one in the isolated model. At even larger radii, the relative difference between the two models is smaller. In the cluster350 model, starting from about 6 Gyr, the SF break stays roughly constant while the SFR is

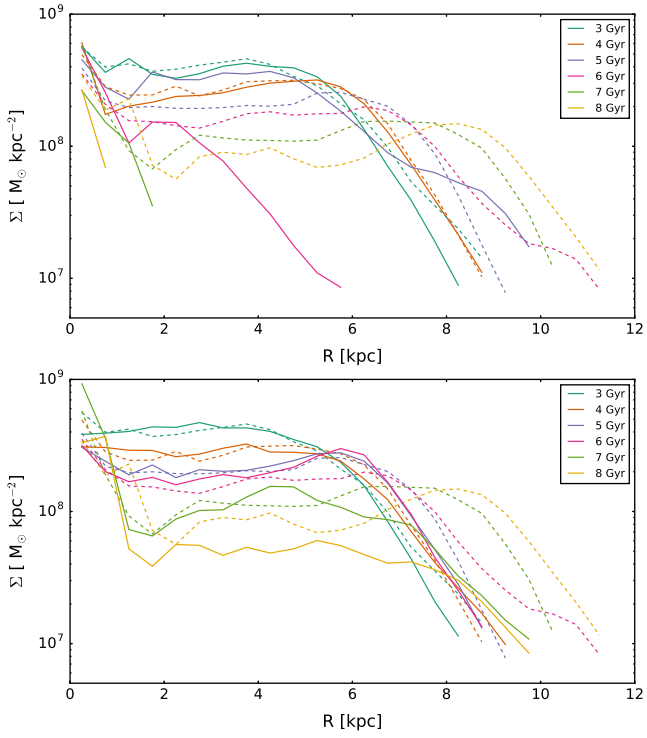

Figure 3. Surface density of young stars (age <0.5 Gyr) as a function of formation radius for the cluster150 model (top panel, solid lines), cluster350 model (bottom panel, solid lines) and the isolated model (dashed lines in both panels) at different times as detailed by the insets.

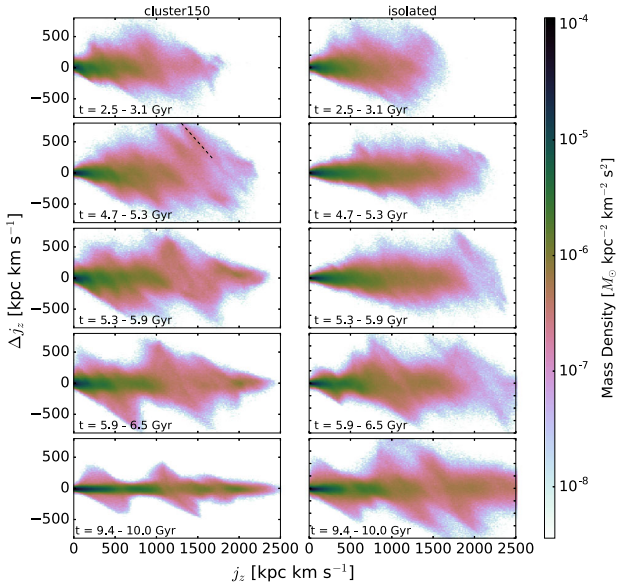

Figure 4. Mass-weighted distributions of Δj_z given starting j_z for the cluster150 model (left) and isolated model (right) at different times. The time intervals at which Δj_z is computed is indicated at the lower left of each panel. The black dashed line (left-hand column, second row) indicates the feature described in the text.

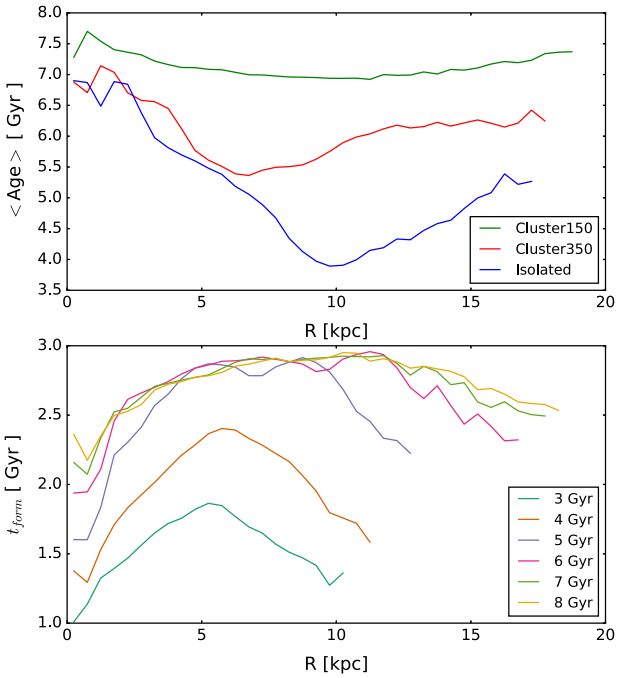

Figure 5. Top panel: mean age profiles for our models at $t = 10$ Gyr as detailed by the inset. Bottom panel: profiles of the evolution of the average formation time of stars for the cluster150 model.

slowly reduced. No significant amount of SF ever occurs outside 6 kpc in this model. Therefore, the presence of stars at $R \sim 15$ kpc in both cluster models requires an explanation.

The bottom panels of Fig. 2 compare the mass-weighted velocity dispersions of the cluster galaxies (black) and the isolated galaxy (red). The cluster galaxies are not substantially hotter, in any direction. For this σ_R, we expect epicyclic excursions to be no larger than $\simeq$3 kpc, since $\Delta R \simeq \sqrt{2}\sigma_R/\kappa$ and taking $\kappa = 25$ km s^{-1} kpc^{-1}. Thus, the presence of stars at large radii in both the cluster150 and the cluster350 models is not due to heating.

Without heating to move stars from the inner to the outer disc, we consider whether the transient spiral migration mechanism of Sellwood & Binney (2002) can explain the presence of these stars in the outer disc. In Fig. 4, we show the change in angular momentum for stars at different times in the cluster150 model (left-hand column) and in the isolated model (right-hand column). In each panel, strong spiral-driven migration manifests as lines of negative gradient (Sellwood & Binney 2002; Roškar et al. 2012). Particles with substantial positive Δj_z have moved outward, whilst particles with negative Δj_z have migrated inward. The top row, at $t = 2.5$–3.1 Gyr, before the onset of significant RPS, shows that at this time the cluster150 and isolated models exhibit grossly similar spiral migration characteristics. By $t = 4.7$–5.3 Gyr, during which time the galaxy passes periapsis, the isolated150 model exhibits the traces of strong, tidally induced spirals in the outer disc. Because these spirals are in the outer disc, there is a substantial asymmetry between outwards and inwards migrators, with the net result of a strong outward migration into the outer disc, which is not present in the isolated model. The outermost feature at this time (indicated by the green dashed line) corresponds to a circular angular momentum $j_c \sim 1850$ kpc km s^{-1} or a corotation radius of $\sim$8 kpc; a $\Delta j_z \sim 600$ kpc km s^{-1} will then move stars out to a radius of $\sim$12 kpc. At this time, this is the extreme outer disc, so migration by tidally induced spirals is likely responsible for populating the outer disc. At later times, spirals in the cluster150 model slowly die out as the quenching of SF robs the disc of the kinematically cool stellar populations needed for sustaining spiral activity (Sellwood & Carlberg 1984). In contrast, SF continues in the isolated model, allowing the disc to grow and spiral activity to persist, permitting its outer disc mass to eventually catch up with that of the cluster150 model.

We also examined similar plots for the cluster350 model, and found that strong, tidally induced outward migrating features are not present to the same extent. Instead, this model is not fully quenched and the continuing SF at intermediate radii feeds the outer disc via the usual spiral migration mechanism.

4 OBSERVATIONAL CONSEQUENCES

In the top panel of Fig. 5, we plot age profiles for the cluster models and the isolated model. As shown by Roškar et al. (2008a), the age profile for the isolated model shows an upturn in average age past the break due to the migration of older stars into the outer disc. In comparison, we find that the cluster150 model shows a flatter average age across the entire disc. The bottom panel shows the evolution of the formation time profile for the cluster150 model in more detail. Until the RPS becomes efficient, the profile has the distinctive down-turn expected from the inside-out growth plus migration mechanism (Roškar et al. 2008b). Once the quenching and tidally induced migration occurs, it rapidly becomes flatter and remains this way throughout. Instead, the cluster350 model exhibits an age minimum at 6 kpc, which is the maximum extent of the high SFR region (though at lower levels SF proceeds beyond this point even to late times).

5 CONCLUSIONS

Using N-body + SPH simulations of galaxies falling into a gas-rich cluster environment, we have shown that gas stripping and tidally induced spirals cause a transition from a type II to a type I profile. Evolved in isolation, the model galaxy develops a type II profile,

whilst the cluster galaxies exhibit either a weakening of the break, or a profile close to that of a type I, depending on the orbital parameters of the galaxy. The radial velocity dispersion is not increased by enough to account for radial excursions of $\Delta R > 10$ kpc needed to populate the outer disc. Instead, we show that there is an increase in spiral activity in the outer disc induced by the cluster potential, causing large outward radial migrations. This efficiently redistributes the material from the inner to the outer disc, while retaining nearly circular orbits (e.g. Sellwood & Binney 2002; Roškar et al. 2012). Whilst observationally few type II profiles are detected in cluster lenticulars (Gutiérrez et al. 2011; Erwin et al. 2012; Roediger et al. 2012), our models retain breaks of varying strength. The cluster simulations presented here have considered only one galaxy in the cluster at a time, whilst in real clusters many galaxies will be present. High-speed tidal interactions between pairs of galaxies may also excite strong spirals in the outer disc (e.g. Moore et al. 1996, 1999), providing the possibility for type I profiles to form in galaxies which do not reach the cluster core, as long as RPS is still able to quench. This can explain why type I profiles are more common amongst cluster lenticulars, but does not explain how they occur in the field. The origin of type I profiles amongst field spiral and lenticular galaxies remains a puzzle. We speculate that interactions between galaxies play a role in the formation of type I profiles in field lenticulars too, together with quenching, which however may not be due to RPS. Whether interactions play any role in type I profiles amongst spiral galaxies remains less clear. NGC 300 is a famous example of a nearby type I spiral galaxy (Bland-Hawthorn et al. 2005). Integrated stellar populations from broad-band colours (Muñoz-Mateos et al. 2007) and *Hubble Space Telescope* resolved stellar populations (Gogarten et al. 2010) find evidence of an inside-out growth, with relatively old ages. Bland-Hawthorn et al. (2005) show that the outer disc has Toomre $Q = 5 \pm 2$, making it unfavourable to strong self-excited spiral structure. Together with its low mass, this makes migration in NGC 300 inefficient (Gogarten et al. 2010). Minchev et al. (2011) invoked NGC 300 as an example of very efficient migration driven by resonance overlap. However, the presence of radial metallicity gradients, in old stars (Gogarten et al. 2010), makes it unlikely that it has experienced extreme migration. Instead type I profiles may be the result of a narrow range of halo angular momenta (Herpich et al. 2015).

Finally, we have shown that in lenticular galaxies the age profile does not show the large upturn expected from the SF threshold and migration mechanism (Roškar et al. 2008b). Instead, the age distribution is quite flat outside the region corresponding roughly to the break-radius at the time of quenching, while inside this region a negative age gradient is present, which is the usual signature of inside-out growth. This provides a testable prediction for our scenario for the formation of type I profiles in cluster lenticulars.

ACKNOWLEDGEMENTS

The simulations in this Letter were run on the COSMOS Shared Memory system at DAMTP, University of Cambridge operated on behalf of the STFC DiRAC HPC Facility. This equipment is funded by BIS National E-infrastructure capital grant ST/J005673/1 and STFC grants ST/H008586/1, ST/K00333X/1. VPD is supported by STFC Consolidated grant # ST/M000877/1.

REFERENCES

Azzollini R., Trujillo I., Beckman J. E., 2008, ApJ, 679, L69
Bakos J., Trujillo I., Pohlen M., 2008, ApJ, 683, L103
Bekki K., 1998, ApJ, 502, L133
Bekki K., Couch W. J., Shioya Y., 2002, ApJ, 577, 651
Binney J., 2004, MNRAS, 347, 1093
Bland-Hawthorn J., Vlajić M., Freeman K., Draine B., 2005, ApJ, 629, 239
Borlaff A. et al., 2014, A&A, 570, A103
Bullock J. S., Dekel A., Kolatt T. S., Kravtsov A. V., Klypin A. A., Porciani C., Primack J. R., 2001, ApJ, 555, 240
Cappellari M. et al., 2011, MNRAS, 416, 1680
Chamaraux P., Balkowski C., Fontanelli P., 1986, A&A, 165, 15
Couch W., Barger A., Smail I., Ellis R., Sharples R., 1998, ApJ, 497, 188
Debattista V. P., Mayer L., Carollo C. M., Moore B., Wadsley J., Quinn T., 2006, ApJ, 645, 209
Dressler A., 1980, ApJ, 236, 351
Dressler A. et al., 1997, ApJ, 490, 577
Drinkwater M. J., Gregg M. D., Colless M., 2001, ApJ, 548, L139
Erwin P., Beckman J., Pohlen M., 2005, ApJ, 626, L81
Erwin P., Pohlen M., Beckman J., 2008, AJ, 135, 20
Erwin P., Gutiérrez L., Beckman J., 2012, ApJ, 744, L11
Foyle K., Courteau S., Thacker R., 2008, MNRAS, 386, 1821
Freeman K., 1970, ApJ, 160, 811
Gogarten S. et al., 2010, ApJ, 712, 858
Gunn J., Gott J., III, 1972, ApJ, 176, 1
Gutiérrez L., Erwin P., Aladro R., Beckman J., 2011, AJ, 142, 145
Herpich J. et al., 2015, MNRAS, 448, L99
Ikebe Y. et al., 1992, ApJ, 384, L5
Larson R. B., Tinsley B. M., Caldwell C. N., 1980, ApJ, 237, 692
Loebman S. R., Roškar R., Debattista V. P., Ivezić Ž., Quinn T. R., Wadsley J., 2011, ApJ, 737, 8
Maltby D., Aragón-Salamanca A., Gray M., Hoyos C., Wolf C., Jogee S., Böhm A., 2015, MNRAS, 447, 1506
Mihos J. C., Hernquist L., 1994, ApJ, 425, L13
Minchev I., Famaey B., 2010, ApJ, 722, 112
Minchev I., Famaey B., Combes F., Di Matteo P., Mouhcine M., Wozniak H., 2011, A&A, 527, A147
Minchev I., Famaey B., Quillen A., Di Matteo P., Combes F., Vlajić M., Erwin P., Bland-Hawthorn J., 2012, A&A, 548, A126
Moore B., Katz N., Lake G., Dressler A., Oemler A., 1996, Nature, 379, 613
Moore B., Ghigna S., Governato F., Lake G., Quinn T., Stadel J., Tozzi P., 1999, ApJ, 524, L19
Muñoz-Mateos J., Gil de Paz A., Boissier S., Zamorano J., Jarrett T., Gallego J., Madore B., 2007, ApJ, 658, 1006
Nasonova O. G., de Freitas Pacheco J. A., Karachentsev I. D., 2011, A&A, 532, A104
Navarro J. F., Frenk C. S., White S. D. M., 1995, ApJ, 462, 22
Pohlen M., Trujillo I., 2006, A&A, 454, 759
Postman M. et al., 2005, ApJ, 623, 721
Pranger F., Trujillo I., Kelvin L., Cebrián M., 2016, preprint (arXiv:1605.08845)
Quilis V., 2000, Science, 288, 1617
Radburn-Smith D. et al., 2012, ApJ, 753, 138
Roediger J., Courteau S., Sánchez-Blázquez P., McDonald M., 2012, ApJ, 758, 41
Roškar R., Debattista V. P., Stinson G. S., Quinn T. R., Kaufmann T., Wadsley J., 2008a, ApJ, 675, L65
Roškar R., Debattista V. P., Quinn T. R., Stinson G. S., Wadsley J., 2008b, ApJ, 684, L79
Roškar R., Debattista V. P., Quinn T. R., Wadsley J., 2012, MNRAS, 426, 2089
Roškar R., Debattista V. P., Loebman S. R., 2013, MNRAS, 433, 976
Schaye J., 2004, ApJ, 609, 667
Sellwood J. A., Binney J. J., 2002, MNRAS, 336, 785
Sellwood J., Carlberg R., 1984, ApJ, 282, 61
Steinhauser D., Schindler S., Springel V., 2016, A&A, 591, A51
Stinson G., Seth A., Katz N., Wadsley J., Governato F., Quinn T., 2006, MNRAS, 373, 1074
Vlajić M., Bland-Hawthorn J., Freeman K., 2011, ApJ, 732, 7
Wadsley J., Stadel J., Quinn T., 2004, New Astron., 9, 137
Younger J., Cox T., Seth A., Hernquist L., 2007, ApJ, 670, 269

This paper has been typeset from a TEX/LATEX file prepared by the author.